In: 2023 AIAA Aviation and Aeronautics Forum and Exposition (AIAA AVIATION Forum), 12-16 June 2023, San Diego, CA
DOI: 10.2514/6.2023-3719

Deep-Learning Methods for Non-Linear Transonic Flow-Field Prediction

Sanjeeth Sureshbabu*, Fernando Tejero†, David MacManus‡, Francisco Sanchez-Moreno§
Centre for Propulsion and Thermal Power Engineering, Cranfield University, Cranfield, MK43 0AL, UK

Christopher Sheaf¶
Installation Aerodynamics Specialist, Rolls-Royce plc

It is envisaged that the next generation of ultra-high bypass ratio engines will use compact aero-engine nacelles. The design and optimisation process of these new configurations have been typically driven by numerical simulations, which can have a large computational cost. Few studies have considered the nacelle design process with low order models. Typically these low order methods are based on regression functions to predict the nacelle drag characteristics. However, it is also useful to develop methods for flow-field prediction that can be used at the preliminary design stages. This paper investigates an approach for the rapid assessment of transonic flow-fields based on convolutional neural networks (CNN) for 2D axisymmetric aero-engine nacelles. The process is coupled with a Sobel filter for edge detection to enhance the accuracy in the prediction of the shock wave location. Relative to a baseline CNN built with guidelines from the open literature, the proposed method has a 75% reduction in the mean square error for Mach number prediction. Overall, the presented method enables the fast prediction of the flow characteristics around civil aero-engine nacelles.

Nomenclature

CFD	=	Computational Fluid Dynamics
CNN	=	Convolutional Neural Network
FNN	=	Fully Connected Neural Network
$FANS$	=	Favre Averaged Navier Stokes
GAN	=	Generative adversarial Networks
LSTM	=	Long Short Term Memory
M	=	Mach
$MFCR$	=	Mass Flow Capture Ratio
MGE	=	Mixed Gradient Error
MLP	=	Multi Layer perceptron
MSE	=	Mean Squared Error
$RANS$	=	Reynolds Averaged Navier Stokes
$UHBPR$	=	Ultra High Bypass Ratio Engines
Y	=	Output

I. Introduction

Computational Fluid dynamics (CFD) methods have been typically used for the design and optimisation of a wide range of aerodynamic components[1]. While RANS-based solvers are the standard for CFD within industry, they are often computationally expensive and time consuming. Within this context, low order models can accelerate the

*Research Assistant in Propulsion Aerodynamics, Propulsion Engineering Centre, Cranfield University
†Lecturer in Propulsion Systems Design, Propulsion Engineering Centre, Cranfield University
‡Head of Gas Turbine Technology Group, Propulsion Engineering Centre, Cranfield University
§PhD candidate, Propulsion Engineering Centre, Cranfield University
¶Installation Aerodynamics, Rolls-Royce plc, Trent Hall 2.2, Derby, DE24 8BJ, UK

overall design process. These are useful at early stages of the design process when it is necessary to perform quick design iterations.

Data-driven low order models such as neural networks offer an approach which significantly reduces the computational cost compared with higher-fidelity CFD evaluations.Within the context of aerodynamic design and optimisation, neural networks are used for the prediction of integral values, the classification of flow-features or the prediction of the flow characteristics around the aerodynamic body of interest. Previous studies have investigated the capabilities of different deep learning architectures for the prediction of flow-fields. For example, Tuliang *et al.* [2] developed a fully connected neural network (FNN) to predict the pressure distribution on supercritical airfoils. A total of 1,500 airfoils shapes were used with a Reynolds number (Re) of Re = $5x10^6$ and a Mach number of 0.76. The model was able to predict the pressure distribution on the upper and lower surfaces of the airfoil with a mean square error on the pressure distribution prediction of $5x10^{-5}$. Important aspects such as pre-shock Mach number or shock location were captured. Hui *et al.* [3] performed a comparative study of the predictive accuracy between FNNs and convolutional neural networks (CNNs). It was based on airfoils and the flow conditions were Re = $6.5x10^6$ and a free-stream Mach number of 0.73. It concluded that the CNN architecture outperforms FNN in predictive accuracy as well as in the required time for training. Guo *et al.* [4] developed a CNN-based model for the prediction of 2D and 3D flow-fields. The study was based on simple geometries at a low Reynolds number of Re = 20. It was demonstrated that for both configurations, i.e. 2D and 3D, the network was able to predict the velocity field. Sekar *et al.* [5] combined FNN and CNN architectures for flow-field prediction around airfoils at low Reynolds number, Re = 500-2500. Within the proposed deep learning architecture, the CNN was used for the geometry parameterization and the FNN for the flow-field estimation. To further improve the accuracy of the current state-of-the-art for flow prediction with low order models, Chen *et al.*[6] proposed a generative adversarial Networks (GAN) [7] architecture. This new method was demonstrated on airfoils and, relative to CNNs, the prediction error was approximately halved from about 4.6% to 2.3%. Deep learning has also been used for flow-field prediction of unsteady flows. For example, Han *et al.* [8] successfully developed a hybrid network involving CNNs and long short-term memory (LSTM) to predict future flow snapshots of the compiled dataset.

Within the context of civil aero-engines, reducing fuel consumption and emissions have been the major driver in the past years[9]. One of the design approaches, by which the next generation of aero-engines aim to meet the Flightpath 2050 targets [10], is to increase the bypass ratio of engines and therefore increase the propulsive efficiency of the engine. The increase in the bypass ratio of the aero-engines may result in larger fan diameters. As such, it is expected that the size of the housing component will increase. If these components are just scaled to accommodate the new fan diameters, this will results in a penalty on weight and overall drag. Consequently it is envisaged that short and compact nacelles will be used to reduce these penalties and to help deliver the benefits of the new engine cycles [11]. However, for transonic conditions with flight Mach number above 0.80 these short and compact nacelles are aerodynamically more sensitive than conventional configurations.The design process for this new challenge has been usually tackled with RANS-based CFD simulations [12][13][14][15]. However, this can have a large computational cost. There is limited information in the open literature in the topic of surrogate modelling for aero-engine nacelles. In addition, the majority of the studies are based on regression-type functions for the prediction of nacelle drag [16]. To complement existing design capabilities with low order models for preliminary nacelle design, it is clear that there is a need to develop rapid methods for flow-field prediction. This will also enable multidisciplinary optimizations were important aspects such as aerodynamic or aerostructural requirements are considered during the design process. In this respect, the novelty of this paper is in the development of a set of convolutional neural networks (CNN) for the flow-field prediction of 2D axisymmetric compact aero-engine nacelles at transonic conditions. Due to the nature of the flow regime considered where shock waves are present, this study incorporates an edge detection method based on a Sobel filter to improve the prediction of the shock location.

II. Methodology

The CFD data used to build convolutional neural networks was generated with a well-established nacelle design and optimisation tool [17][16] . A thorough description of the framework has been provided in the past [17][16] and, as such, only a brief description is provided below (Section II.A). For this work, the existing nacelle design method (Figure 1) has been extended to accommodate a capability to build convolutional neural network upon which fast flow-field predictions of 2D axisymmetric aero-engine nacelles can be performed (Section II.B).

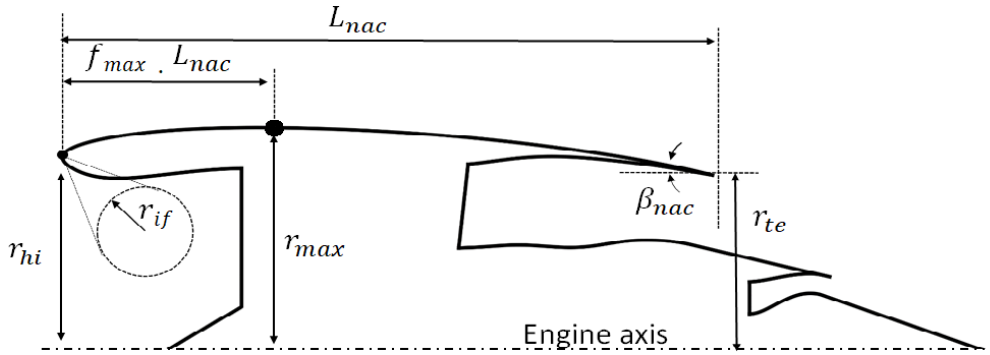

(a) Design variables for a 2D axisymmetric aero-engine nacelle

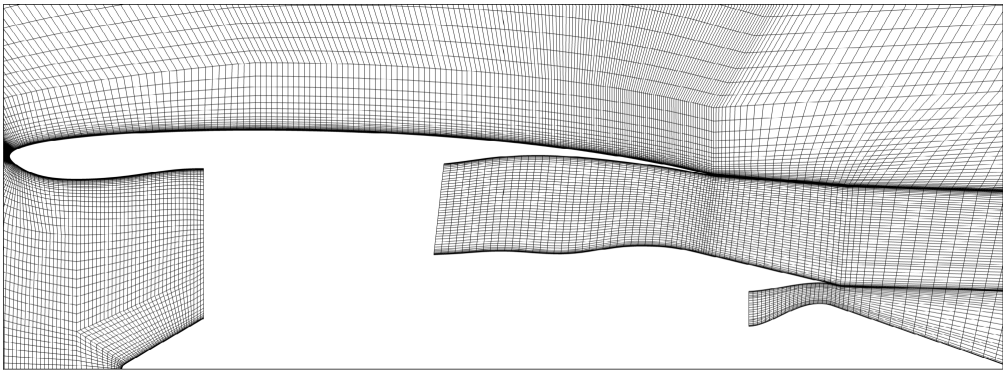

(b) Computational mesh

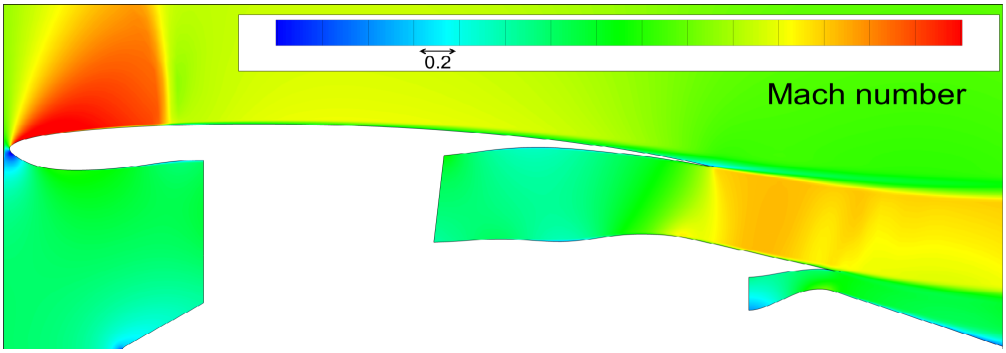

(c) CFD solution

Fig. 1 Overview of the CFD workflow for 2D axisymmetric aero-engine nacelles

A. Nacelle design and optimisation framework

The aero-engine nacelle geometry of a 2D aero-line is controlled with a parametric definition based on the intuitive Class Shape Transformation (iCST) method [18]. Each nacelle aero-line is defined with 7 parameters: $r_{max}, f_{max}, r_{if}, \beta_{nac}$, L_{nac}, r_{hi} and r_{te} (Figure 1a). During the nacelle design process the variables of L_{nac}, r_{hi}, r_{te} are usually fixed and the remaining ones, i.e $r_{max}, f_{max}, r_{if}, \beta_{nac}$, float.

The computational domain is generated with a multi-lock structured meshing approach in which the farfield is located at $80r_{max}$. The selection of the domain size is based on a previous domain sensitivity study [17]. The first cell height is adjusted to $y^+ = 50$. The overall cell count was approximately 70k cells. A grid independence study was performed based on Roache's method [19], in which three grid sizes with approximately 35, 70 and 140 were considered. For typical mid-cruise conditions for transonic applications with Mach number of 0.85 and massflow capture ratio of 0.7, the grid convergence index was of about 0.04% on nacelle drag normalised with the net thrust for the reference mesh with 70k cells.

The CFD simulations were carried out with a double-precision density based solver and the k-ω SST[20] model was used as turbulence closure. Ideal gas properties were used and the viscosity was calculated with Sutherland's law [21]. The farfield boundary condition was set with a pressure-farfield in which it is imposed the Mach number and the static temperature and pressure associated to the flight altitude. The fan-face was modelled with a pressure-outlet in which a target massflow is specified to meet the required MFCR. The core and bypass duct inlets were modelled with a pressure inlet condition where total temperature and pressure are set. The intake, spinner, nacelle, bypass, core and plug walls were modelled with a non-slip boundary condition.

B. Convolutional Neural Network method

Neural networks are function approximators that map an input to an output through a set of neurons. For an input vector $\mathbf{x}$ and output vector $\mathbf{y}$, a simple single neuron neural network can be defined as Eq. 1:

$$\mathbf{y} = \sigma(\mathbf{x} * W) \tag{1}$$

Where w is a weighting factor and σ is an activation function [22]. The weights of the neurons are learnt during the training process. The activation function enables the neural network to model complex and non-linear functions. There are a wide range of neural network architectures that have been investigated in the past for flow-field prediction [2][3]. Within this work, convolutional neural networks (CNN) are used to predict the flow-field of aero-engine nacelles.

Convolutional neural networks have been widely used in image processing, object recognition, image reconstruction and super resolution. They are efficient in handling tensor type data and they make efficient use of GPUs which reduces the overall training time. The sparse connectivity of CNN as compared to multilayer perceptrons reduces also the memory requirements. To predict flow-field around aero-engine nacelles, the CNN uses the geometric shape as input and outputs the flow-field prediction. The architecture follows a encoding-decoding network (Figure 2). The encoding part consists of convolutional layers to extract information from the input and encodes it into a low dimensional space. This convolutional network is then followed by a fully connected layer. The decoding network consists of inverse convolutional layers known as deconvolutional layers. They decode the low dimensional geometrical information to produce flow-field predictions.

An important aspect of training a convolutional neural network is pre-processing the data. It is important to note that as part of a CFD workflow, all the flow-field quantities are calculated in the cells of the computational domain. The distance between cells across the mesh is not uniform as larger refinement will be usually targeted near the non-slip walls. However, for the CNN architecture the data has to be resampled into a uniform structured grid. For this purpose, a Cartesian grid with an axial extent of $3L_{nac}$ and radial extent of $3r_{hi}$ was used with a resample of 100x200 pixels (Figure 3). Previous studies have used a binary definition of the pixels in which pixels located in the fluid domain received a value of 1, and pixels outside of the fluid domain received a value of 0. However, recent work from Guo *et al.* [4] demonstrated that using signed distance functions (SDF) improve the CNN's accuracy. This method is based on assigning to each pixel the minimum orthogonal distance to the boundary of the domain (Figure 3). Based on this evidence, this work uses the signed distance function (Eq. 2) as input of the developed CNNs.

$$SDF = \begin{cases} 0 & x \in (\partial\Omega, \Omega) \\ -d(x, \partial\Omega) & x \notin \Omega \end{cases} \tag{2}$$

where x indicates each pixel and Ω represents the aero-engine nacelle boundaries.

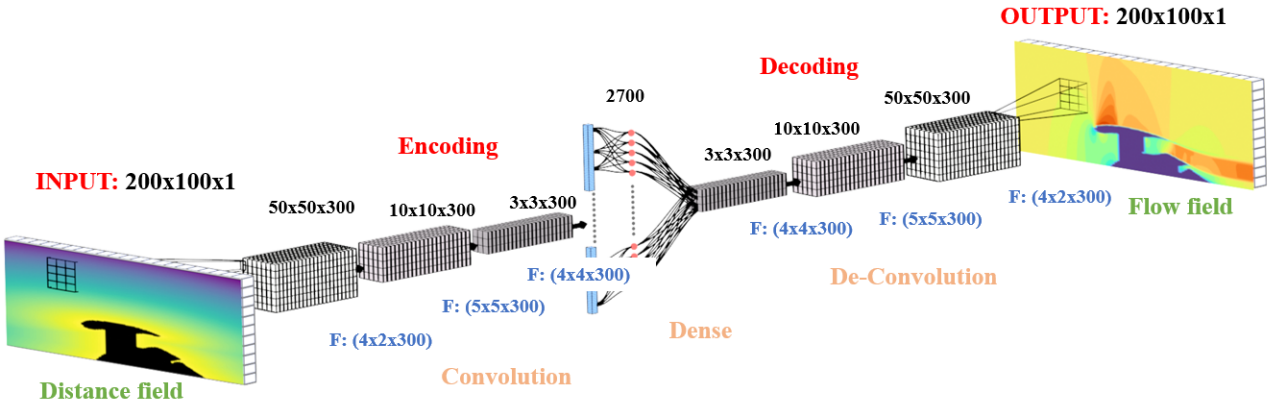

Fig. 2 Architecture of a baseline CNN

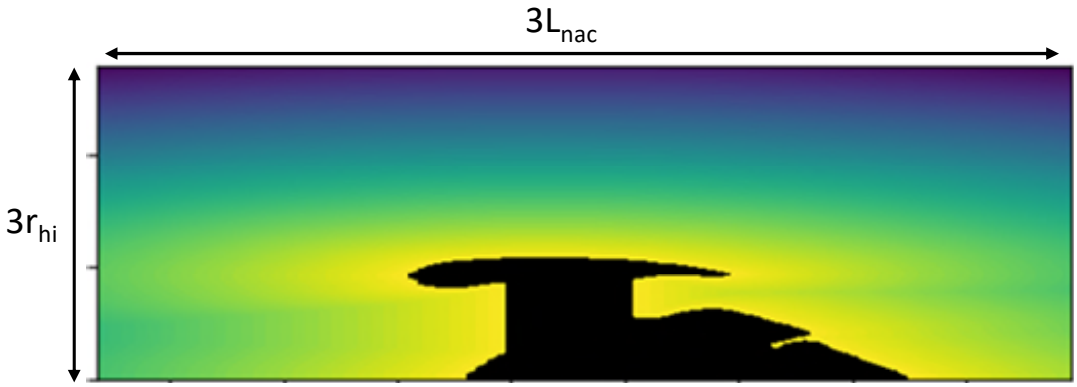

Fig. 3 Example of signed distance function (SDF) that is used as input of the CNN

The main objective of this work is to assess the capabilities of convolutional neural networks for the flow-field prediction of aero-engine nacelles at transonic conditions. For this purpose, the CNNs were only trained to predict Mach number. However, it is important to note that the architectures could be easily extended to other flow properties. Whilst this work focuses on the flow-field characteristics around the nacelle, the CNNs should also predict the intake flow as well as the transonic exhaust flow. During the training process of the CNNs, the mean square error (MSE) of the Mach number prediction was used as the loss function (Eq. 3).

$$MSE = \frac{1}{n}\sum_{i=1}^{n}(Y_{CFD} - Y_{CNN})^2 \tag{3}$$

III. Results

This work investigates the design space for compact aero-engine nacelles with L_{nac}/r_{hi} = 3.1. This is a short configuration that is expected for future turbofan architectures [16]. Previous studies have highlighted the large aerodynamic non-linearity of this design space. As such, it represents a significant challenge for flow-field prediction with low order models. The aerodynamic analysis is carried out for a typical mid-cruise condition of long-range

applications with M = 0.85 and MFCR = 0.7, and the 2D nacelle aero-line is defined with the 4 intuitive degrees of freedom of r_{max}, f_{max}, r_{if} and β_{nac} (Figure 1a). A database was compiled based on a design exploration with a Latin hypercube sampling technique. A total number of 400 designs were gathered in which the 80% were used to train the different convolutional neural network models and the remaining ones, i.e. 20%, were employed to assess the predictive accuracy of the developed CNNs.

It is important to note that different flow characteristics are encountered across the investigated design space. For transonic conditions, different shock structures may be generated along the nacelle. This poses significant challenges for flow-field prediction with low order models. To provide an initial insight of the different flow-fields that are expected in the considered design space, Figure 4 presents the transonic characteristics of two different architectures. The first aero-engine has a strong initial acceleration around the lip with a large peak isentropic Mach number which terminates in a strong shock on the nacelle forebody. The second configuration has an initial weak shock wave in the nacelle forebody and the flow gradually accelerates to terminate in a second shock at the nacelle afterbody.

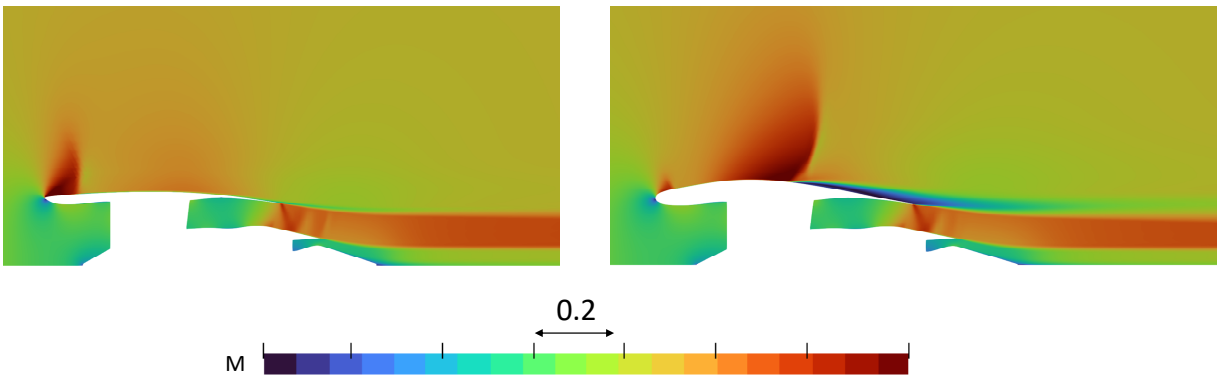

Fig. 4 Contour of Mach number for two aero-engine nacelles in the training dataset

A. Baseline convolutional neural network (CNN-1)

This work uses as baseline CNN, also refereed as CNN-1 throughout the text, an architecture based on the work performed by Guo *et al.* [4] and Bhatnagar *et al.* [23] with an encoding-decoding network approach. For the encoder, the input size was 100x200x1 (length x width x depth) as per the data resampling in the Cartesian grid (Figure 3). The input layer is followed by 3 convolutional layers of filters (4,2),(5,5) & (4,4), with strides of (4,4), (5,5), (4,2), respectively. The output of the encoder is flattened into a single column of length 2700 elements. This is connected to the deconvolutional network, which is composed by 3 fully connected layers. The final output layer of the CNN architecture is of size 100x200x1 and provides predictions of Mach number. A filter size of 300 was used for all layers of the architecture (Figure 2). In addition, the ReLu activation function was used on all the layers (Eq. 4).

$$f(x) = max(0, x) \tag{4}$$

The convolutional neural network was trained with Tensorflow [22]. As previously discussed, overall 320 samples were used for training the CNN and around 80 for validation purposes. The trained convolutional neural network resulted in a mean square error in the validation database of MSE = 0.0027. Having trained the baseline CNN, flow-field predictions for unseen aero-engine nacelles were carried out. Figure 5 compares the CFD and CNN prediction for four designs (D1, D2, D3 and D4) which have different flow characteristics. The configuration D1 presents a well defined shock at the nacelle aft-body. Conversely, the nacelles D2 and D4 has a single shock at the nacelle forebody with a significant difference on the initial acceleration around the nacelle lip. Lastly, the architecture D3 has a double shock structure. Across the wide range of nacelles, the CNN method can predict the main flow characteristics associated to these configurations. However, there are changes in the shock location which highlights the limitations of the baseline convolutional neural network (CNN-1). In particular, the largest discrepancy appears for the design D2 (Figure 5). A quantification of the differences between the CFD and the predicted flow-field is presented in the next Section.

Although the hyperparameters used in the baseline CNN were derived from a previous work, it is important to note that an important aspect of training deep learning architectures is to adequately select the hyperparameters that

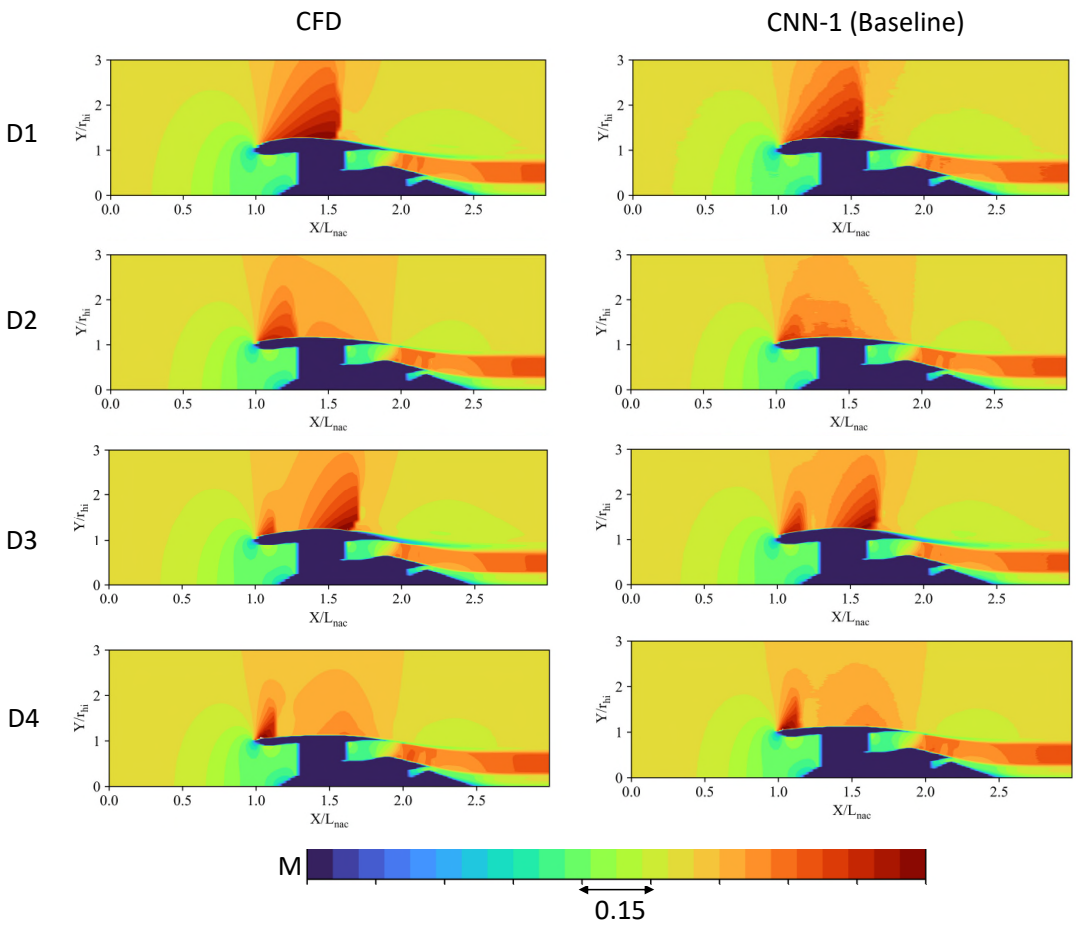

Fig. 5 Mach number comparison between CFD and the baseline CNN for 4 selected aero-engine nacelles

define the low order model. In this respect, a hyperparameter study was undertaken to improve the performance of the convolutional neural network for flow-field prediction in aero-engine nacelle applications. Overall, 4 different hyperparameters were consider: activation function, number of filters, batch normalization and loss function. For this work, a full factorial combination of the different set of hyperparameters was not performed. Instead, changes in the baseline CNN were performed by only changing one of the hyperparameters. Then, the final deep learning architecture was built on the basis of using the hyperparameters with the best accuracy of each perturbation performed with the 4 hyperparemeters. One important aspect when defining a deep learning architecture is to define the activation function, which ensures that non-linearities of the problem are captured by the neural network. Whilst the activation function used by the baseline network was ReLu (Eq. 4), two other activation functions were tested: leaky ReLu (Eq. 5) and tanh (Eq. 6). Previous work with artificial neural networks to predict the nacelle drag of compact aero-engines considered ReLu, tanh and sigmoid as activation functions [24]. It was found that ReLu outperformed tanh and sigmoid. For flow-field prediction and CNN architectures, similar trend was found where ReLu and tanh had a MSE of 0.0027 and 0.0160, respectively (Figure 6a). For this work, leaky ReLu was also considered due to its proven capabilities to model non-linear data. This resulted in a mean square error in the prediction of Mach number of MSE = 0.00092.

$$f(x) = max(0.01x, x) \tag{5}$$

$$f(x) = tanh(x) \tag{6}$$

Within the context of building convolution neural networks, other important hyperparameter is the number of filters at each layer. Whilst a large number of filters can result in high accuracy of the metamodel, it can also lead to overfitting.

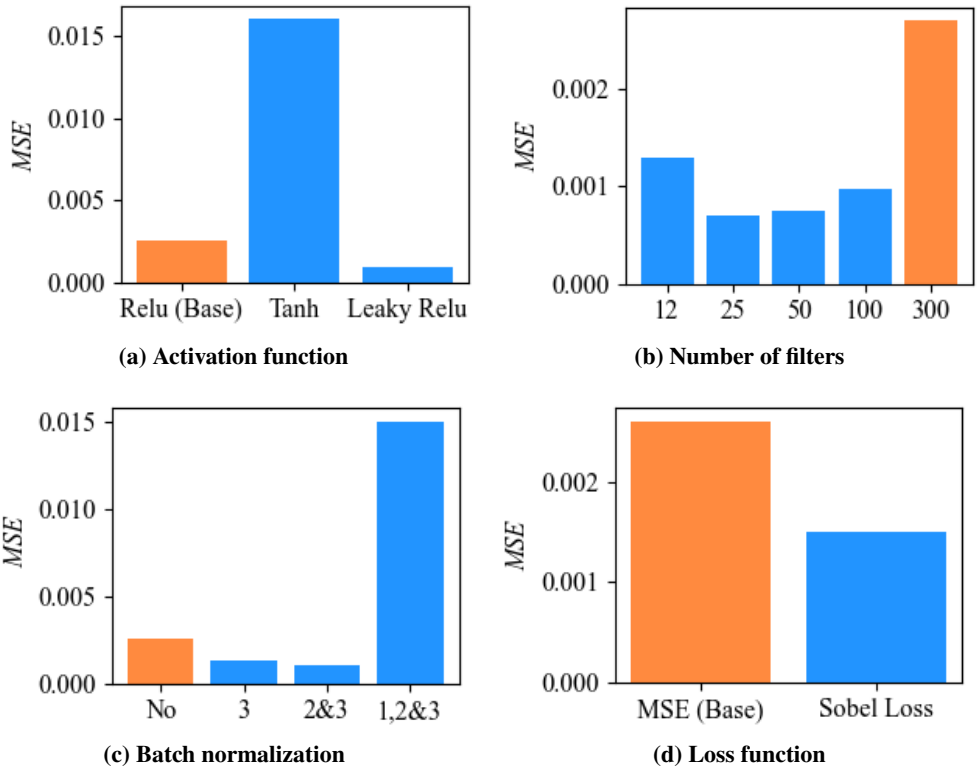

(a) Activation function **(b) Number of filters**

(c) Batch normalization **(d) Loss function**

Fig. 6 Effect of hyperparameter on CNN accuracy for Mach number prediction. The orange bar indicates the baseline CNN-1 architecture

As such, it is important to identify the adequate trade-off. To cover a wide range, the number of filters in each layer was varied from 12 to 300. For the CNN built with 12 filters, the MSE was 0.0013. The mean square error reduced to 0.00070 when the number of filters was increased to 25 (Figure 6b). A further increment in the number of filters results in a worse CNN with MSE = 0.00075. Subsequently, as the number of filters was increased the accuracy of the CNN was reduced with a maximum value of MSE = 0.0027 for the baseline CNN that used 300 filters (Figure 2). Other parameters that was considered to improve the accuracy of the CNN was the batch normalization, which is used to normalize the output of each layer by re-centering and re-scaling the data. This reduces the covariance during the training process and can result in a performance improvement of the network [4]. Whilst the baseline CNN did not use batch normalization, this technique was used in a series of combinations for the deconvolutional layers. In this respect, three different configurations were considered in which batch normalization was only applied to the third, i.e. last, layer (DeCN3), to the second and third layers (DeCN 2 & 3) and to all the deconvolutional layers (DeCN 1, 2 & 3). Relative to the baseline CNN that was not using the batch normalization technique, the DeCN3 and DeCN 2 & 3 CNN architectures presented an improvement on the model accuracy with a mean square error on the Mach number prediction of 0.0014 and 0.00105, respectively (Figure 6c). Whilst this showed that this hyperparameter is useful to further improve the accuracy, it is also important to note that it can also degrade it. For example, using batch normalization in the three deconvolutional layers (DeCN 1, 2 & 3) resulted in a MSE of 0.015 (Figure 6c) compared to MSE = 0.00105 for the DeCN 2 & 3 CNN architecture.

Other hyperparameter used to further improve the CNN's accuracy was the loss function. The baseline CNN used the mean square error (MSE), which is a metric that has been used in the past for a range of applications [4] [24]. It measures the difference between the CNN prediction and the higher fidelity CFD data. However, this loss function may not be the best suited for transonic applications with shock-waves. This is because of the flow-field discontinuities created by the shocks, which may result in large errors associated with small changes in the prediction of the shock location. For this reason, this work also uses a Sobel filter in the loss function to enhance the prediction in regions where high flow gradient are located. Sobel filters have been used in the past for edge detection in image processing. Lu *et al.* [25] used a Mixed Gradient Error (MGE) based loss function which combined Sobel filter in the loss function with the

standard MSE. This was successfully demonstrated to improve the accuracy of super resolution models to enhance image sharpness at the edges. For this work, the new loss function used to train the CNNs is defined as in Eq. 7:

$$Loss = MSE + \lambda_G MGE \tag{7}$$

where λ_G is a weight term. For this work λ_G was set to 0.1. The MGE term (Eq. 8) is defined as:

$$MGE = \frac{1}{n}\frac{1}{m}\sum_{i=1}^{n}\sum_{j=1}^{m}(G(i,j) - \hat{G}(i,j))^2 \tag{8}$$

where n and m represent the horizontal and vertical pixels (data points) in the image, i.e. flowfield. The term $G(i, j)$ is the convolution of X- and Y-Sobel filters (Eq. 9 and 10) to the flow-field data.

$$G_x = Y * \begin{bmatrix} -1 & -2 & -1 \\ 0 & 0 & 0 \\ 1 & 2 & 1 \end{bmatrix} \tag{9}$$

$$G_y = Y * \begin{bmatrix} -1 & 0 & 1 \\ -2 & 0 & 2 \\ -1 & 0 & 1 \end{bmatrix} \tag{10}$$

Where Y represents the image data, i.e. flow-field, and '*' represents the convolution operation of the filter over the image array. The x and y filtered data is combined by Eq. 11:

$$G(i,j) = \sqrt{(G_x^2(i,j) + G_y^2(i,j))} \tag{11}$$

The incorporation of this filter enhanced the prediction of shocks by the network and reduced the mean square error to MSE = 0.0015 (Figure 6d).

B. Final convolutional neural network (CNN-2)

A final network (CNN-2) was built based on the previous parametric study which quantified the impact of the different hyperparameters on the predictive accuracy of the metamodels. The CNN-2 model was built with the Leaky ReLu activation function, a total of 25 number of filters, the deconvolutional layers two and three used batch normalisation and the network was trained using a Sobel filter approach (Figure 6). This resulted in a convolutional neural network with a mean square error on Mach number prediction of MSE = 0.00065 for the independent dataset with approximately 80 designs. This is a reduction of approximately 75% compared to the baseline CNN (Section III.A). Other improvement of the new CNN-2 model was that the training time was reduced by approximately a factor of 10. This was achieved, primarily, by the large reduction of the number of filters used in the different layers of the model. Figure 7 presents the Mach number prediction for the 4 selected aero-engine nacelles that have associated different flow characteristics. For comparison purposes, the four configurations, i.e. D1, D2, D3 and D4, are the same as the ones presented in Figure 5. For the D1 nacelle, the CNN-2 model shows a good agreement with CFD. A similar level of agreement was also obtained for the baseline CNN-1 (Figure 5). The transonic flow-field characteristics associated to D2, D3 and D4 are also well predicted by CNN-2. However, the baseline CNN-1 model failed to capture the shock location (Figure 5). It highlights that the developed deep learning architecture CNN-2 is suitable for modelling complex flow-fields for transonic applications.

To quantify the benefits of the CNN-2 deep learning architecture relative to the baseline CNN, Figure 8 shows the error on the Mach number prediction for the four downselected designs. As commented above, both CNN architectures presented a similar prediction for the nacelle D1 for which the shock location and its intensity is well-predicted. It is important to note that the largest errors appear near the wall due to the limitations of CNN architectures near the edges of the domain [3]. Larger differences appear for the configuration D2 and D4 in which the shock location was not captured by the baseline CNN-1 model but was well approximated by the developed CNN-2 architecture. Similar finding was identified for D3 for which the baseline deep learning architecture failed to capture both shock locations but CNN-2 successfully captures them. This highlights the capabilities of the developed CNN architecture for complex non-linear data. Whilst the predictive capability developed in this work is successfully demonstrated for this problem, it

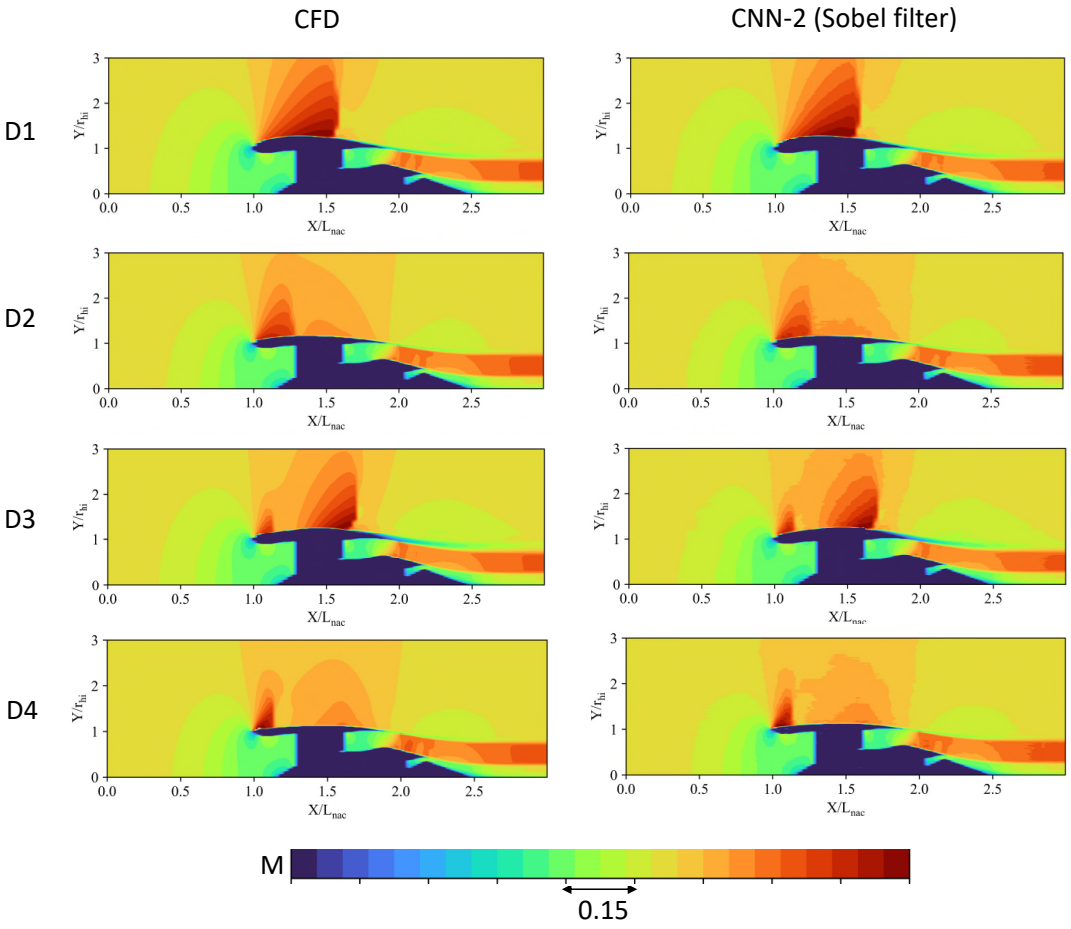

Fig. 7 Mach number comparison between CFD and CNN-2 for 4 selected aero-engine nacelles

is also important to note that it has limitations. The approach can successfully predict the main flow characteristics associated to aero-engine nacelles. However, it is important to highlight that the errors near the wall are relatively high (Figure 8). As such, future work should focus on the improvement of the deep learning architecture to ensure higher resolution near the wall to allow, for example, accurate drag extraction from the predicted flow-field.

IV. Conclusions

A deep learning model based on convolutional neural networks (CNN) has been successfully developed for flow-field prediction on aero-engine nacelles with a flight Mach number of 0.85. Relative to a baseline CNN built with guidelines from the open literature, the proposed architecture has a 75% reduction in the mean square error for Mach number predictions. This has been achieved by fine-tuning different hyperparameters that have a large impact on the model accuracy. A new loss function that uses a Sobel filter approach has been implemented to ensure that shock locations and their intensity are better predicted. This is a key aspect for the transonic conditions considered in this work. In addition, the overall training time of the new CNN has been reduced by a factor 10 due to the simplified architecture proposed. Overall, it is demonstrated that the developed approach is suitable for the prediction of the non-linear transonic flow-fields associated to aero-engine nacelles. Future work will focus on improving the flow-field prediction near the wall boundaries to ensure that the boundary layer characteristics are better captured by the deep learning models.

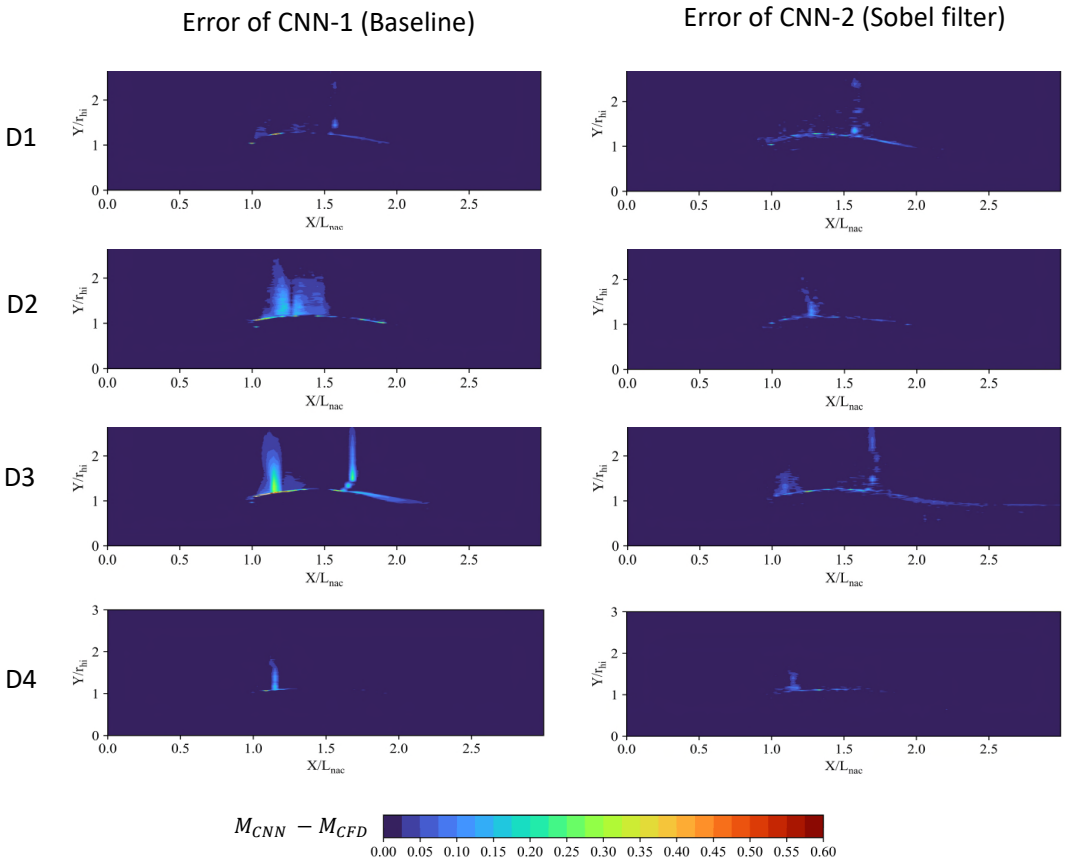

Fig. 8 Error on Mach number prediction for the D1, D2, D3 and D4 aero-engine nacelles

Acknowledgments

The authors thank Rolls-Royce plc for supporting this research

Data availability statement

Due to commercial confidentiality agreements the supporting data are not available.

References

[1] Martins, J. R., "Aerodynamic design optimization: Challenges and perspectives," *Computers & Fluids*, Vol. 239, 2022, p. 105391.

[2] Tuliang, M., Hairun, X., and Jing, W., "Pressure distribution prediction of supercritical airfoils at multiple flight conditions using deep learning approach," *Journal of Physics: Conference Series*, Vol. 2292, IOP Publishing, 2022, p. 012012.

[3] Hui, X., Bai, J., Wang, H., and Zhang, Y., "Fast pressure distribution prediction of airfoils using deep learning," *Aerospace Science and Technology*, Vol. 105, 2020, p. 105949.

[4] Guo, X., Li, W., and Iorio, F., "Convolutional neural networks for steady flow approximation," Association for Computing Machinery, 2016, pp. 481–490.

[5] Sekar, V., Jiang, Q., Shu, C., and Khoo, B. C., "Fast flow field prediction over airfoils using deep learning approach," *Physics of Fluids*, Vol. 31, 2019.

[6] Chen, D., Gao, X., Xu, C., Chen, S., Fang, J., Wang, Z., and Wang, Z., "FlowGAN: A conditional generative adversarial network for flow prediction in various conditions," IEEE Computer Society, 2020, pp. 315–322.

[7] Goodfellow, I. J., Pouget-Abadie, J., Mirza, M., Xu, B., Warde-Farley, D., Ozair, S., Courville, A., and Bengio, Y., "Generative Adversarial Networks," *Advances in Neural Information Processing Systems*, 2014.

[8] Han, R., Wang, Y., Zhang, Y., and Chen, G., "A new prediction method of unsteady wake flow by the hybrid deep neural network," *Computational Mechanics*, Vol. 33, 2019.

[9] Birch, N. T., "2020 vision: the prospects for large civil aircraft propulsion," *The Aeronautical Journal*, Vol. 104, 2000, pp. 347–352.

[10] Commission, E., "Flightpath 2050: Europe Vision for Aviation, Tech. Rep. 978-92-79-19724-6, Publications Office of the European Union," , 2011.

[11] Tejero, F., MacManus, D., Matesanz-Garcia, J., Swarthout, A., and Sheaf, C., "Towards the Design and Optimisation of Future Compact Aero-Engines: Intake/Fancowl Trade-Off Investigation," *International Journal of Numerical Methods for Heat & Fluid Flow*, 2022.

[12] Schreiner, D., Tejero, F., Macmanus, D. G., and Sheaf, C., "Robust aerodynamic design of nacelles for future civil aero-engines," *ASME TurboExpo 2020, GT2020-14470*, 2020.

[13] Swarthout, A., MacManus, D., Tejero, F., Matesanz-García, J., Boscagli, L., and Sheaf, C., "A comparative assessment of multi-objective optimisation methodologies for aero-engine nacelles," *33rd Congress of the International Council of the Aeronautical Sciences (ICAS)*, 2022.

[14] Sanchez-Moreno, F., MacManus, D., Tejero, F., Matesanz-Garcia, J., and Sheaf, C., "Robustness of optimisation algorithms for transonic aerodynamic design," *9th European Conference for Aeronautics and Space Sciences (EUCASS-3AF)*, 2022.

[15] Goulos, I., MacManus, D., Hueso-Rebassa, J., Tejreo, F., Au, A., and Sheaf, C., "Impact of installation on the performance of an aero-engine exhaust at wind-milling flow conditions," *ASME TurboExpo 2023, GT2023-100833*, 2023.

[16] Tejero, F., MacManus, D. G., and Sheaf, C., "Surrogate-based aerodynamic optimisation of compact nacelle aero-engines," *Aerospace Science and Technology*, Vol. 93, 2019.

[17] Tejero, F., Robinson, M., MacManus, D. G., and Sheaf, C., "Multi-objective optimisation of short nacelles for high bypass ratio engines," *Aerospace Science and Technology*, Vol. 91, 2019, pp. 410–421.

[18] Tejero, F., MacManus, D., Hueso-Rebassa, J., Sanchez-Moreno, F., Goulos, I., and Sheaf, C., "Aerodynamic Optimisation of Future Civil Aero-Engines by Dimensionality Reduction and Multi-Fidelity Techniques," *International Journal of Numerical Methods for Heat & Fluid Flow*, 2022.

[19] Roache, P., "A method for uniform reporting of grid refinement studies," *Journal of Fluids Engineering*, Vol. 116 (3), 1994, pp. 405–413.

[20] Menter, F., "Two-Equation eddy-viscosity turbulence models for engineering applications," *AIAA Journal*, Vol. 32, 1994.

[21] Sutherland, W., "The viscosity of gases and molecular force," *Philosophical Magazine Series 5*, Vol. 36, 1893, pp. 507–531.

[22] Abadi, M., and et al., "TensorFlow: Large-scale machine learning on heterogeneous systems," 2015. Software available from tensorflow.org.

[23] Bhatnagar, S., Afshar, Y., Pan, S., Duraisamy, K., and Kaushik, S., "Prediction of aerodynamic flow fields using convolutional neural networks," *Computational Mechanics*, Vol. 64, 2019, pp. 525–545.

[24] Tejero, F., MacManus, D., Sanchez, F., and Sheaf, C., "Neural network-based multi-point, multi-objective optimisation for transonic applications," *Aerospace Science and Technology*, 2023.

[25] Lu, Z., and Chen, Y., "Single Image Super Resolution based on a Modified U-net with Mixed Gradient Loss," *Signal, Image and Video Processing*, Vol. 16, 2, p. 1143–1151.

2023-05-08

Deep-learning methods for non-linear transonic flow-field prediction

Sureshbabu, Sanjeeth

AIAA

Sureshbabu S, Tejero F, Sanchez-Moreno F, et al., (2023) Deep-learning methods for non-linear transonic flow-field prediction. In: 2023 AIAA Aviation and Aeronautics Forum and Exposition (AIAA AVIATION Forum), 12-16 June 2023, San Diego, CA

https://doi.org/10.2514/6.2023-3719